

Pressure coefficient analysis for a setback building

Vedprakash Sharma^{1a}, Shubham Singh^{1a}, Sourabh Sangwan^{1a} & Hrishikesh Dubey^{2*}

*Corresponding Author: Hrishikesh.dubey@dtu.ac.in

Abstract- The design of tall buildings is heavily influenced by wind flow characteristics which pose a greater challenge to designers, engineers, and architects. For understanding the wind loads and their effects on the building Computational Fluid Dynamics (CFD) tools are widely used. This paper focuses on the Coefficient of pressure along the circumference at two different elevations for a 7.5% setback provided from all sides at two different elevations using the k- ϵ model. For the validation of this study, the analysis is first done over a rectangular calibrated model with the same height and base area as that of the setback model and the results of the pressure coefficient are compared with the Indian standard code IS 875 (Part 3): 2015. Variation of C_{pe} along circumference is observed with a change in wind incident angle from 0 ° to 90 ° for an interval of 30°.

Key words:- Setback building, angle of incidence, wind pressure coefficient, computational fluid dynamics

Introduction

In the current scenario due to rapid urbanization, increasing population, and limited availability of land resources, there is an increase in demand for high-rise buildings. Previously high-rise buildings were of regular shapes but there is a shift to irregular shapes for better architecture. Tall buildings produce more challenges for designers due to large wind exposure. So aerodynamic optimization becomes important with other design aspects (Lin et al., 2005a; Xie, 2012). There are different ways of analyzing wind-induced effects on the buildings one such method of analysis is the wind tunnel experiment (Amin & Ahuja, 2013). The wind tunnel experiment gives accurate results but is expensive and time taking. CFD tools are another method for the analysis which is relatively cheaper and less time consuming and gives comparable results to that of wind tunnel experiment (Bhattacharyya & Dalui, 2014). CFD tools are multifaceted and vibrant (Blocken, 2014), hence they are very useful for studying the complex aerodynamics of complex structures (Ding et al., 2014). Various researchers have performed wind effect analysis on different shapes of buildings such as, L-shape buildings (Kumar & Raj, 2022), Y plan shaped

<http://dx.doi.org/10.55953/JERA.1101>

buildings (Goyal et al., 2022), U and L shape structures (Gomes et al., 2005), square and fish-plan shape tall buildings (Pal et al., 2021), L and T shaped models (Amin & Ahuja, 2011), cross shape tall buildings (Raj Ahirwar et al., 2013), plus-shaped buildings (Raj et al., 2018) and irregular octagonal (oval) shape building (Kumar & Raj, 2021).

Numerous forms of setback structures (Y. C. Kim et al., 2019; Y. Kim & Kanda, 2010; Lin et al., 2005b; Rajasekarababu & Vinayagamurthy, 2019; Sharma et al., 2019a; Xu et al., 2017) have been studied at various levels. A wind tunnel experiment on tapered and set-back buildings had been conducted by Kim and Kanda with 5% and 10% tapering ratios and concluded that tapered and setback models lead to a decrease in fluctuating lift force and mean drag force (Y. Kim & Kanda, 2010). Gehlot found out that theirs a direct relation in height to width ratio and peak pressure coefficient on the windward face model by analysing different surfaces for change in wind pressure coefficient with varying height to width ratio of tapered high-rise buildings (Gehlot, 2015). Kumar Bairagi et al. found out that in comparison to tall buildings setback buildings have higher values of pressure, turbulence and spectral density by analysing the dynamic behaviour and pressure on the building for varied wind incidence angles on a CFD simulation of tall setback buildings (Kumar Bairagi & Ku Mar Dalui, 2018). Sharma et al. conducted a study for tapered and setback building finding values of moments, mean along wind forces and RMS across wind forces significantly reduced for setback building as compared to a tapered building (Sharma et al., 2019b).

In this paper, the study on setback building is discussed to understand the wind-induced effect on building under atmospheric boundary layer (ABL) conditions using the study of coefficient of pressure distribution along the circumference on the faces of the building model with a varying AOI of wind at three different elevations. For this study, a setback model of 1 m height is taken with a plan area of 300 mm X 200 mm with two 7.5% setbacks provided from each side. This analysis has been performed on Ansys CFX software. Standard k- ϵ model has been used for the analysis. This study will help in ensuring the aerodynamic stability of tall buildings for different wind AOI.

MODEL DESCRIPTION

The model used in the study is a setback building having two setbacks of 7.5% from each side. The model is scaled down by 450 times to a height of 1m in Ansys CFX software with the actual height of the building being 450 m. The height of the model is 1 m with a base floor area of 300 mm \times 200 mm and subsequent deck areas of 255 mm \times 170 mm and 216.75 mm \times 144.5 mm as shown in figure 1. As per the guidelines given by (Franke, 2007) the domain inlet, sides and outlet are at 5H, 5H and 15H respectively from the faces of the building and the

top is at 6H from the ground where H is the height of the model as shown in Figure 2. The detailed study of the model is done at wind incident angles of 0°, 30°, 60° and 90°.

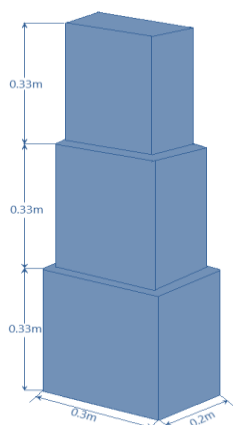


Fig:1 Set Back Model

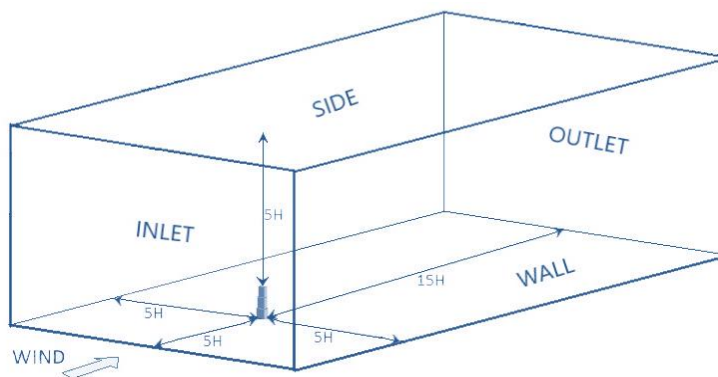


Fig:2 Computational Domain

COMPUTATIONAL GRID AND BOUNDARY CONDITIONS

Meshing used for the domain is in a tetrahedral pattern, as advised by Chakraborty et al (Chakraborty et al., 2014). For better results, the meshing of the building model is finer than that of the computational domain. Twenty layers of inflation are provided for the model as shown in fig 4. The number of nodes and elements are 89,792 and 4,56,482 respectively. The model faces and ground surface of the domain are taken as a no-slip wall ($u_{wall} = 0$) and the sidewalls are taken as free slip walls ($\tau_{wall} = 0, u_{wall} = 0$). τ_{wall} and u_{wall} represent fluid shear stress on the wall and components of fluid velocity normal to the wall respectively. The power law is used to attain homogeneous steady wind flow under ABL conditions.

Power law: -

$$U = \frac{U_{ref}}{(z/z_{ref})^\alpha} \tag{1}$$

Where z_{ref} is the boundary layer depth, u_{ref} is the boundary layer velocity and α is a function of terrain roughness. The boundary layer velocity (U_{ref}) is taken as 10m/s, Terrain roughness coefficient (α) as 0.143 and Z_{ref} as 1m

The velocity profile at the inlet is parabolic as shown in figure 3.

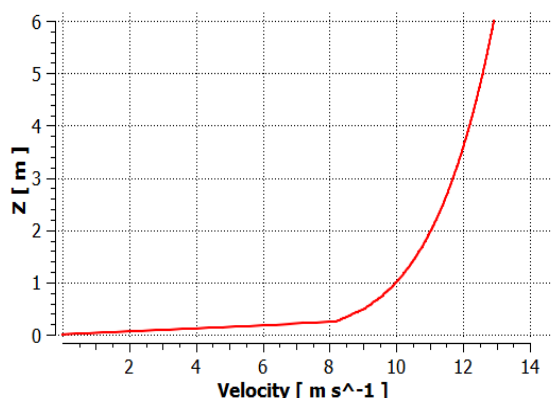


Figure 3. Velocity profile

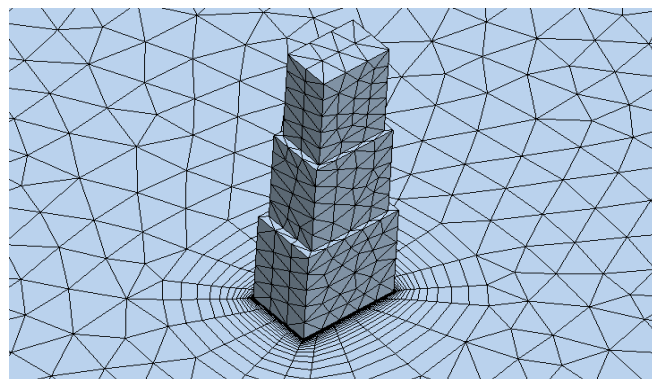


Figure 4. Meshing

In this paper k- ε model is used in Ansys CFX for analysis.

VALIDATION

For the validation of this study, a rectangular calibrated model of the same height and base area as that of the setback building model is used. The dimensions of the calibrated model are 300 mm × 200 mm × 1000 mm (L × B × H). The input parameters and boundary conditions are kept the same. The coefficient of pressure (C_{pe}) values on the faces of calibrated model are compared with the Indian standard code (IS: 875 (Part 3): 2015) (IS:875. (2015). Indian Standard design loads (other than earthquake) for Buildings and Structures. Part 3: Wind Loads (Third Revision)., 2015) and the values are found to be well within the acceptable range as shown in table 1.

As per	Wind Angle	Face A	Face B	Face C	Face D
Ansys CFX	0°	0.66	-0.41	-0.68	-0.68
	90°	-0.57	-0.58	0.56	-0.35
IS: 875 (Part 3): 2015	0°	0.7	-0.4	-0.7	-0.7
	90°	-0.5	-0.5	0.8	-0.1

Table 1. C_{pe} values at face A, B, C and D for calibrated model

RESULTS AND DISCUSSION

The variation of pressure coefficient along the circumference at different elevations is analysed over four wind incident angles (0°, 30°, 60°, and 90°).

C_{pe} along Circumference

The variation of C_{pe} along the circumference in the horizontal direction for setback buildings having 7.5% setback from $0^\circ, 30^\circ, 60^\circ$, and 90° is shown in figure 5 and 6. For 0° wind AOI, the pressure coefficient on the windward face shows almost positive values on all three decks because the windward face receives direct streamlines. The leeward and side faces show negative pressure coefficient values. The peak negative pressure coefficient shows high suction pressure. High suction pressure occurs at leading edges and corners. The C_{pe} along the leeward faces is almost uniform due to the formation of vortices and generation of the wake region. Positive C_{pe} values are observed on windward faces on all three decks with a slight variation due to an increase in the intensity of the wind along with the height. On leeward and side faces large variations in C_{pe} values are observed due to an increase in the frequency of vortices along with the height. Negative C_{pe} values are observed over side faces due to strong viscous shear force and suction.

For 90° AOI wind pressure coefficient follows the same pattern as that for 0° wind AOI. The windward face shows positive C_{pe} values due to direct velocity streamlines on it. Leeward and side faces show negative C_{pe} due to suction, vortex formation, and wake region. The C_{pe} values along with circumference change significantly for other wind incidence angles. For 30° and 60° AOI, large variations of mean pressure coefficient are observed for face A and face C due to the high-velocity gradient. The maximum positive and maximum negative values of C_{pe} are observed for 0° and 90° AOI. The values of maximum and minimum C_{pe} over different faces for 0° and 90° AOI are shown in 6. From the C_{pe} along with the circumference graph, it is observed that both maximum and minimum C_{pe} values increase with an increase in the setback.

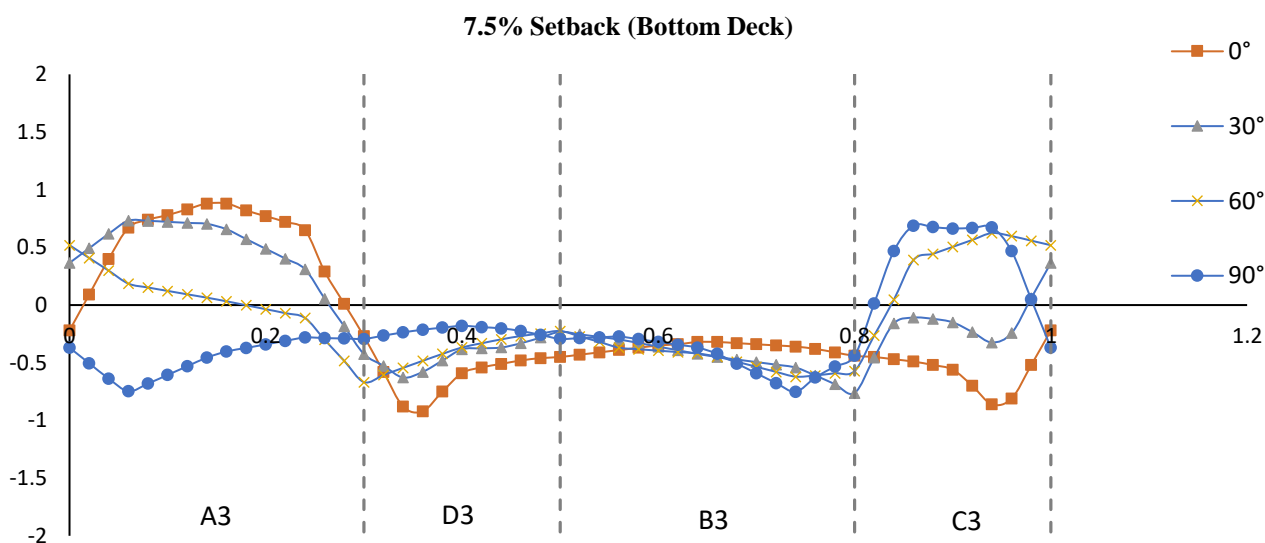


Figure 5 (a). Variation of Cpe along perimeter at Z = 0.167 m

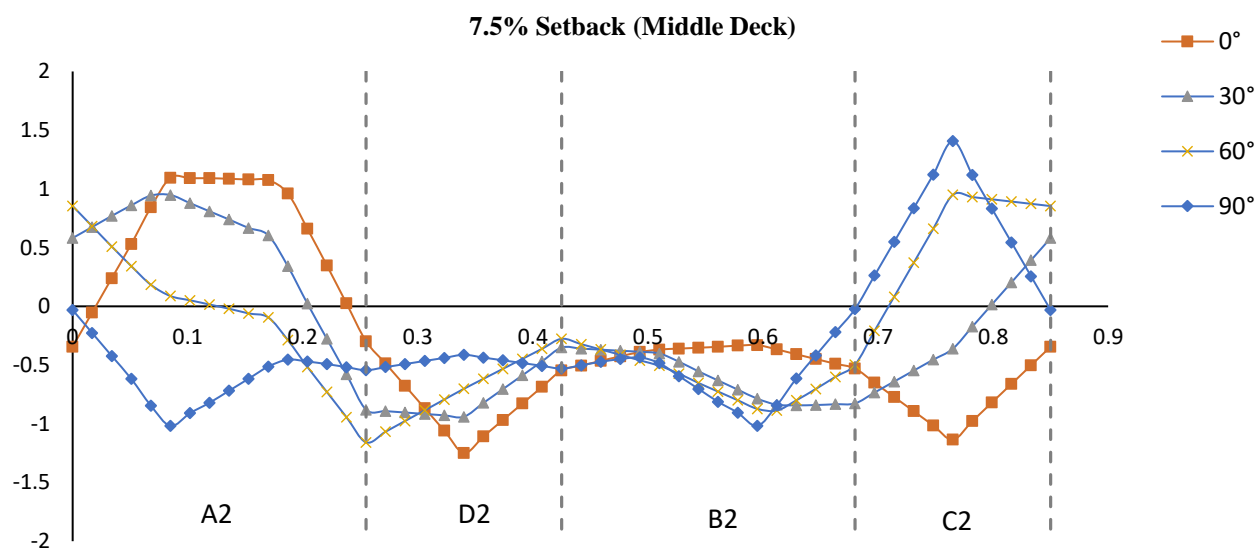


Figure 5 (b). Variation of Cpe along perimeter at Z = 0.5 m

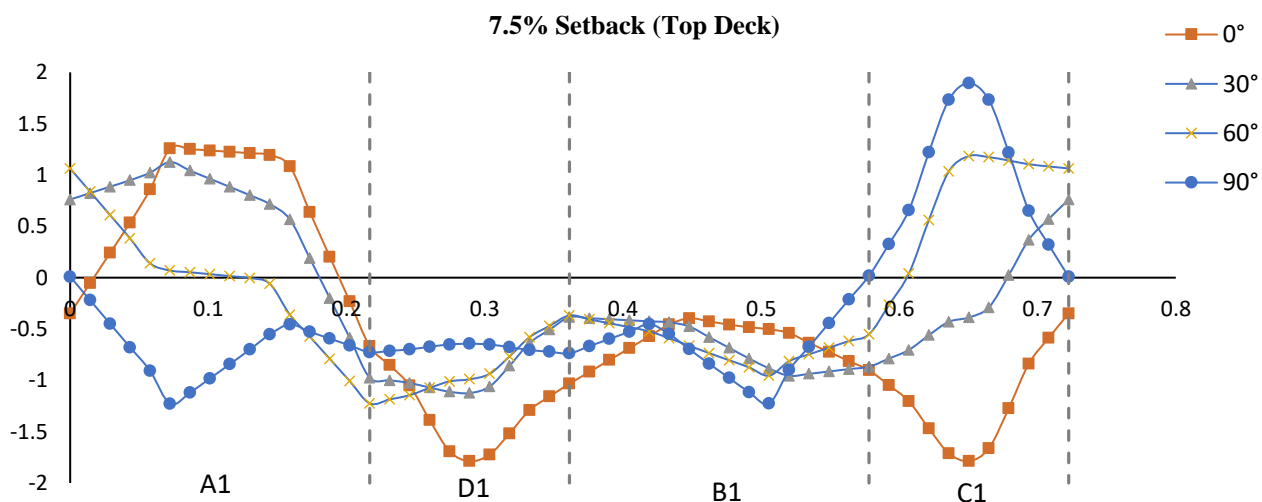


Figure 5 (c). Variation of Cpe along perimeter at Z = 0.833 m

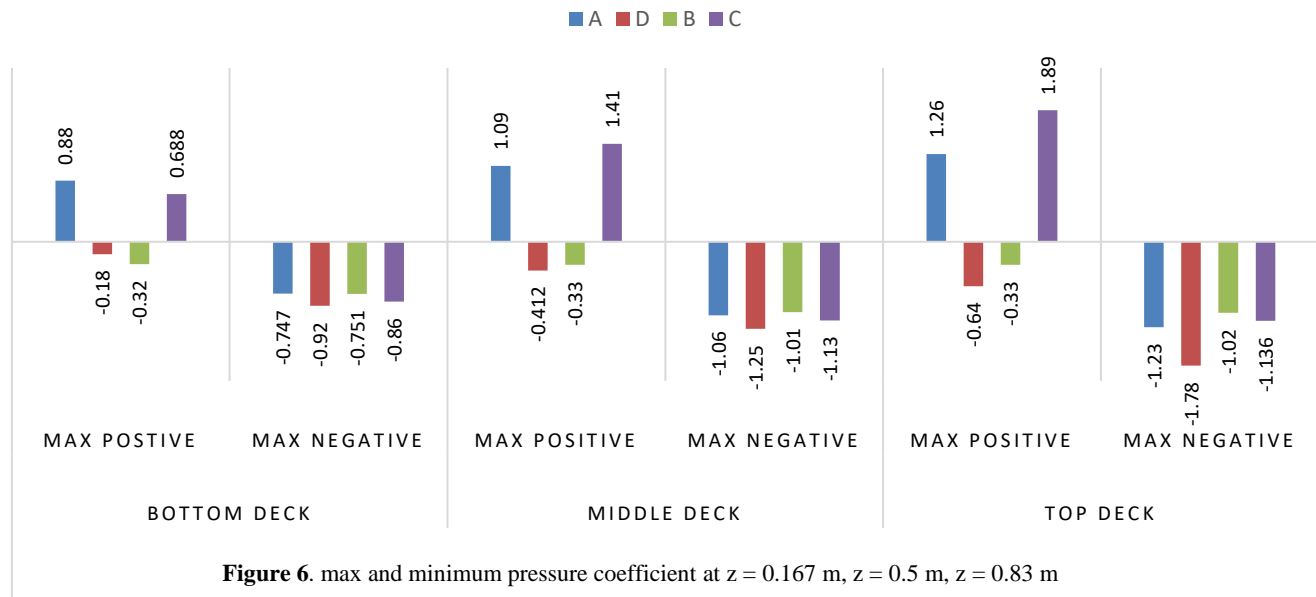


Figure 6. max and minimum pressure coefficient at $z = 0.167$ m, $z = 0.5$ m, $z = 0.83$ m

CONCLUSIONS

The major conclusions from the present study are as follows: -

- Variation of C_{pe} along the circumference with change in AOI shows that the maximum C_{pe} value of 1.89 is obtained on face C1 for 90° AOI and the minimum C_{pe} value of -1.78 is obtained on face D1 for 0° AOI and both maximum and minimum values are obtained on the top deck. This also shows that the faces having less contact area with the wind show higher C_{pe} values.
- With the change in AOI from 0° to 90° pressure coefficient values on the side and leeward faces do not change significantly as compared to windward faces.

Data Availability Statement

All data, models and code generated or used during the study appear in the submitted article.

Funding Statement

Authors would like to express their sincere gratitude to Delhi Technological University, Delhi, India for providing research facilities to conduct this research work.

Acknowledgments:

The authors acknowledge the Department of Civil Engineering and Delhi Technological University, Delhi

Conflict of Interest:

The authors declare that there are no conflicts of interest.

REFERENCES

1. Amin, J. A., & Ahuja, A. K. (2011). Experimental study of wind-induced pressures on buildings of various geometries. In *International Journal of Engineering, Science and Technology* (Vol. 3, Issue 5). www.ijest-ng.com
2. Amin, J. A., & Ahuja, A. K. (2013). Effects of Side Ratio on Wind-Induced Pressure Distribution on Rectangular Buildings. *Journal of Structures*, 2013, 1–12. <https://doi.org/10.1155/2013/176739>
3. Bhattacharyya, B., & Dalui, S. K. (2014). *Comparative study between regular and irregular plan-shaped tall building under wind excitation by numerical technique*. <https://doi.org/10.13140/2.1.1689.9202>
4. Blocken, B. (2014). 50 years of Computational Wind Engineering: Past, present and future. *Journal of Wind Engineering and Industrial Aerodynamics*, 129, 69–102. <https://doi.org/10.1016/J.JWEIA.2014.03.008>
5. Chakraborty, S., Dalui, K., & Ahuja, A. K. (2014). Experimental Investigation of Surface Pressure on “+” Plan Shape Tall Building. In *Jordan Journal of Civil Engineering* (Vol. 8, Issue 3).
6. Ding, W., Uematsu, Y., Nakamura, M., & Tanaka, S. (2014). Unsteady aerodynamic forces on a vibrating long-span curved roof. *Wind and Structures, An International Journal*, 19(6), 649–663. <https://doi.org/10.12989/was.2014.19.6.649>
7. Franke, J. , H. A. , S. H. , & C. B. (2007). *Proceedings / International Workshop on Quality Assurance of Microscale Meteorological Models Cost action 732 in combination with the European Science Foundation at Hamburg, Germany, July 28/29, 2005*.
8. Gehlot, K. P. (2015). Numerical Analysis of Wind loads on Tapered Shape Tall Buildings. In *IJSTE-International Journal of Science Technology & Engineering /* (Vol. 1, Issue 11). www.ijste.org

<http://dx.doi.org/10.55953/JERA.1101>

9. Goyal, P. K., Kumari, S., Singh, S., Saroj, R. K., Meena, R. K., & Raj, R. (2022). Numerical Study of Wind Loads on Y Plan-Shaped Tall Building Using CFD. *Civil Engineering Journal*, 8(2), 263–277. <https://doi.org/10.28991/cej-2022-08-02-06>
10. IS:875. (2015). Indian Standard design loads (other than earthquake) for Buildings and Structures. Part 3: Wind Loads (Third Revision). (2015). *IS-875-part-3-2015*.
11. Kim, Y., & Kanda, J. (2010). Characteristics of aerodynamic forces and pressures on square plan buildings with height variations. *Journal of Wind Engineering and Industrial Aerodynamics*, 98(8–9), 449–465. <https://doi.org/10.1016/J.JWEIA.2010.02.004>
12. Kumar, A., & Raj, R. (2021). Study of pressure distribution on an irregular octagonal plan oval-shape building using cfd. *Civil Engineering Journal (Iran)*, 7(10), 1787–1805. <https://doi.org/10.28991/cej-2021-03091760>
13. Kumar, A., & Raj, R. (2022). CFD Study of Flow Characteristics and Pressure Distribution on Re-Entrant Wing Faces of L-Shape Buildings. *Civil Engineering and Architecture*, 10(1), 289–304. <https://doi.org/10.13189/cea.2022.100125>
14. Kumar Bairagi, A., & Ku Mar Dalui, S. (2018). *Aerodynamic Effects on Setback Tall Building Using CFD Simulation Aerodynamic shape modification of “Y” plan shaped tall building*. <https://www.researchgate.net/publication/325711150>
15. Pal, S., Raj, R., & Anbukumar, S. (2021). Comparative study of wind induced mutual interference effects on square and fish-plan shape tall buildings. *Sadhana - Academy Proceedings in Engineering Sciences*, 46(2). <https://doi.org/10.1007/S12046-021-01592-6>
16. Raj Ahirwar, R., Raj, R., & Kumar Ahuja, A. (2013). Wind Loads on Cross Shape Tall Buildings Wind effects on tall buildings View project Response of Closely Spaced Tall Buildings under Wind Loads View project Wind Loads on Cross Shape Tall Buildings. *Journal of Academia and Industrial Research*, 2(2). <https://www.researchgate.net/publication/352781701>
17. Raj, R., Sharma, A., & Chauhan, S. (2018). *Response of Square and Plus Shaped Buildings on Varying Wind Loads*. 206–215. <https://doi.org/10.1061/9780784482032.022>
18. Rajasekarababu, K. B., & Vinayagamurthy, G. (2019). Experimental and computational simulation of an open terrain wind flow around a setback building using hybrid turbulence models. *Journal of Applied Fluid Mechanics*, 12(1), 145–154. <https://doi.org/10.29252/jafm.75.253.29179>
19. Sharma, A., Mittal, H., & Gairola, A. (2019a). Wind-induced forces and flow field of aerodynamically modified buildings. *Environmental Fluid Mechanics*, 19(6), 1599–1623. <https://doi.org/10.1007/s10652-019-09687-9>



<http://dx.doi.org/10.55953/JERA.1101>

20. Xie, J. (2012). *The Seventh International Colloquium on Bluff Body Aerodynamics and its Applications (BBAA7) Aerodynamic optimization in super-tall building designs*. <https://doi.org/2012>.

Received: 25 February 2022

Revised: 05 April 2022

Accepted: 22 April 2022

Journal of Engineering Research and Application

